Timelike and Spacelike DVCS: NLO Corrections and their importance

Lech Szymanowski

National Centre for Nuclear Research (NCBJ), Warsaw

CEA Saclay, 25-27 November 2013

Outline

DVCS

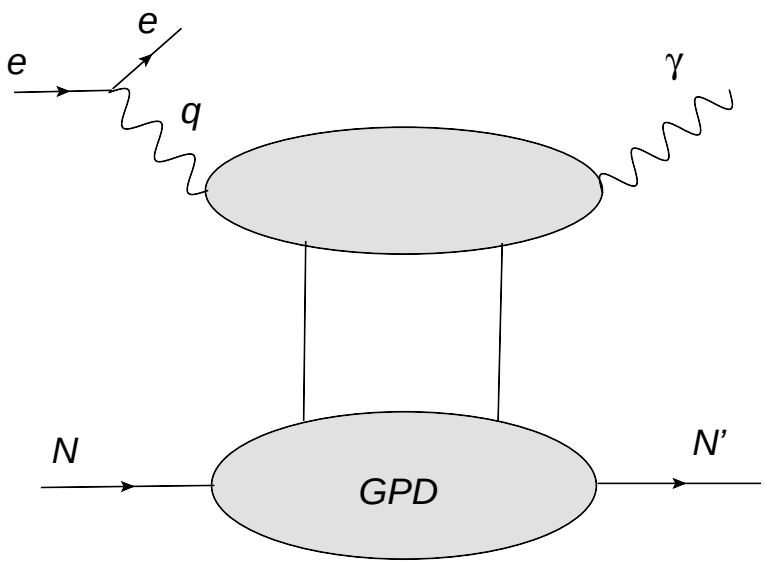

Figure: Deeply Virtual Compton Scattering : $lN \to l'N'\gamma$

Skewness ξ:

$$\xi = -\frac{(P' - P)n}{(P + P')n}$$

TCS

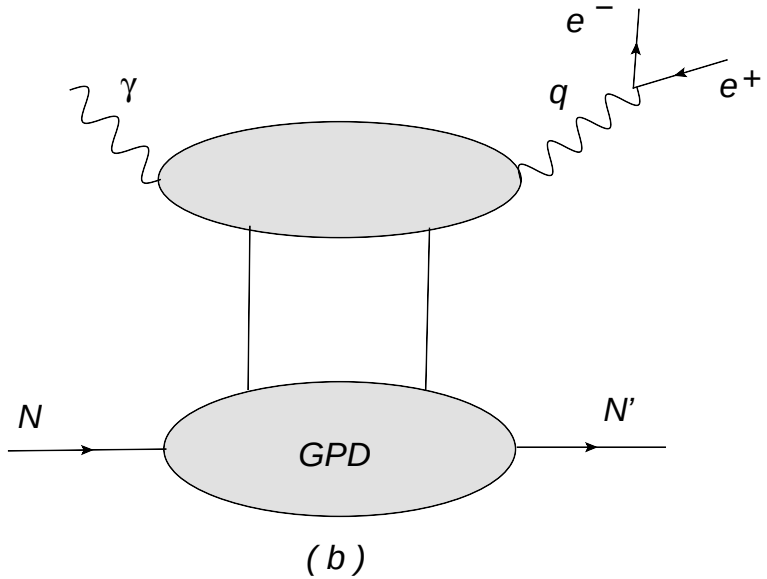

Figure: Timelike Compton Scattering: $\gamma N \to l^+ l^- N'$

Skewness η:

$$\eta = -\frac{(P' - P)n}{(P + P')n}$$

Why TCS?

- GDPs enter factorization theorems for hard exlusive reactions (DVCS, deeply virtual meson production, TCS etc.), in a similar manner as PDFs enter factorization theorem for DIS
- First moment of GPDs enters the Ji's sum rule for the angular momentum carried by partons in the nucleon,
- Deeply Virtual Compton Scattering (DVCS) is a golden channel for GPDs extraction,
- Why TCS: universality of the GPDs, spacelike-timelike crossing and understanding the structure of the NLO corrections,
- Experiments *at low energy*: CLAS 6 GeV $\rightarrow$ CLAS 12 GeV, *at high energy*: COMPASS, RHIC, LHC (and AFTER@LHC).

Coordinates

Berger, Diehl, Pire, 2002

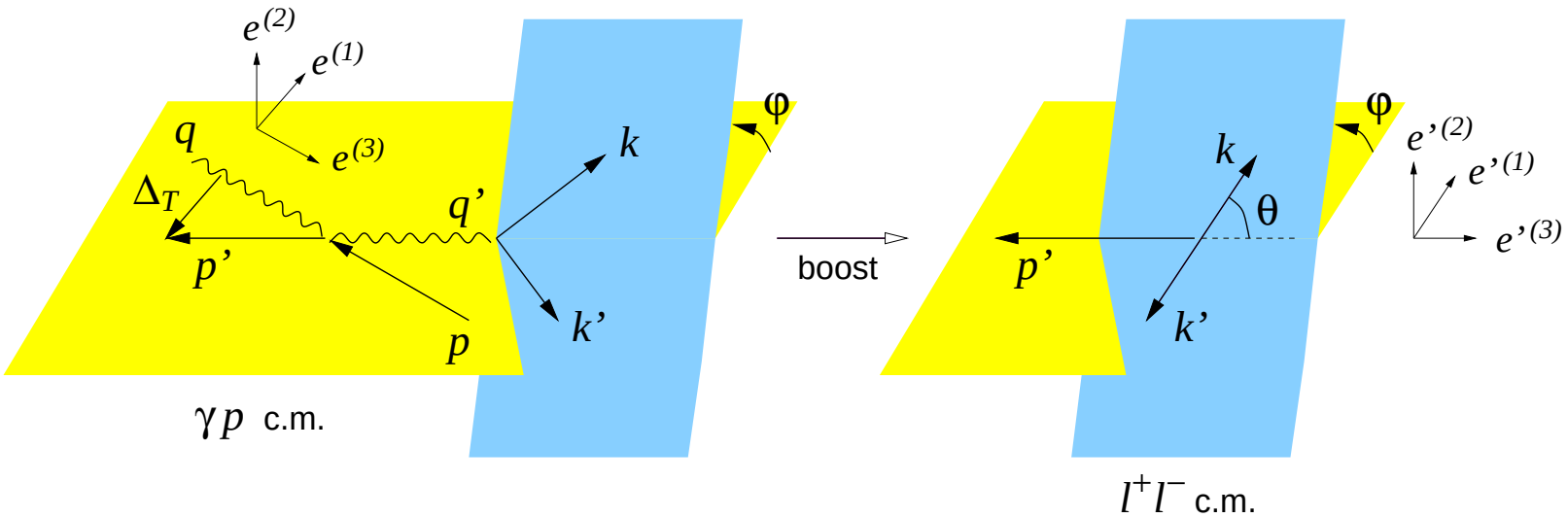

Figure: Kinematical variables and coordinate axes in the γp and $\ell^+\ell^-$ c.m. frames.

The Bethe-Heitler contribution

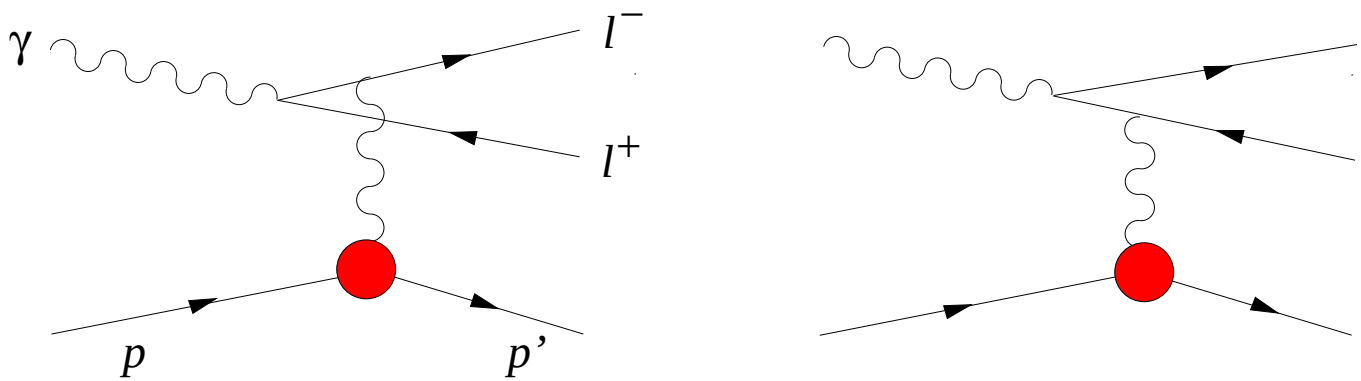

Figure: The Feynman diagrams for the Bethe-Heitler amplitude.

$$\frac{d\sigma_{BH}}{dQ'^2 dt d\cos\theta} \approx 2\alpha^3 \frac{1}{-tQ'^4} \frac{1+\cos^2\theta}{1-\cos^2\theta} \left(F_1(t)^2 - \frac{t}{4M_p^2} F_2(t)^2 \right),$$

For small θ BH contribution becomes very large

The Compton contribution

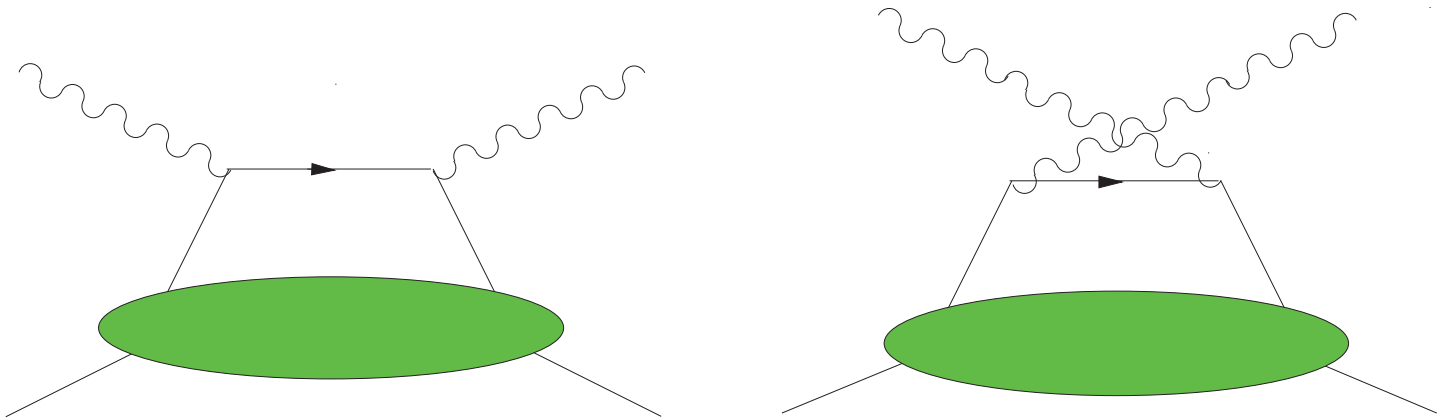

Figure: Handbag diagrams for the Compton process in the scaling limit.

$$\frac{d\sigma_{TCS}}{dQ'^2 d\Omega dt} \approx \frac{\alpha^3}{8\pi}\frac{1}{s^2}\frac{1}{Q'^2}\left(\frac{1+\cos^2\theta}{4}\right)2(1-\xi^2)\left|\mathcal{H}(\xi,t)\right|^2,$$

$$\mathcal{H}(\xi,t) \quad = \quad \sum_q e_q^2 \int_{-1}^{1} dx T(x,\xi,Q') H^q(x,\xi,t),$$

Compton Form Factor

Interference

The interference part of the cross-section for $\gamma p \to \ell^+ \ell^- p$ with unpolarized protons and photons is given at leading order by

$$\frac{d\sigma_{INT}}{dQ'^2\, dt\, d\cos\theta\, d\varphi} \sim \cos\varphi\ \mathrm{Re}\,\mathcal{H}(\xi, t)$$

Linear in GPD's, odd under exchange of the l^+ and l^- momenta $\Rightarrow$ angular distribution of lepton pairs is a good tool to study interference term.

Berger, Diehl, Pire, 2002

B-H dominant for small energies;

JLAB 6 GeV data

Rafayel Paremuzyan PhD thesis

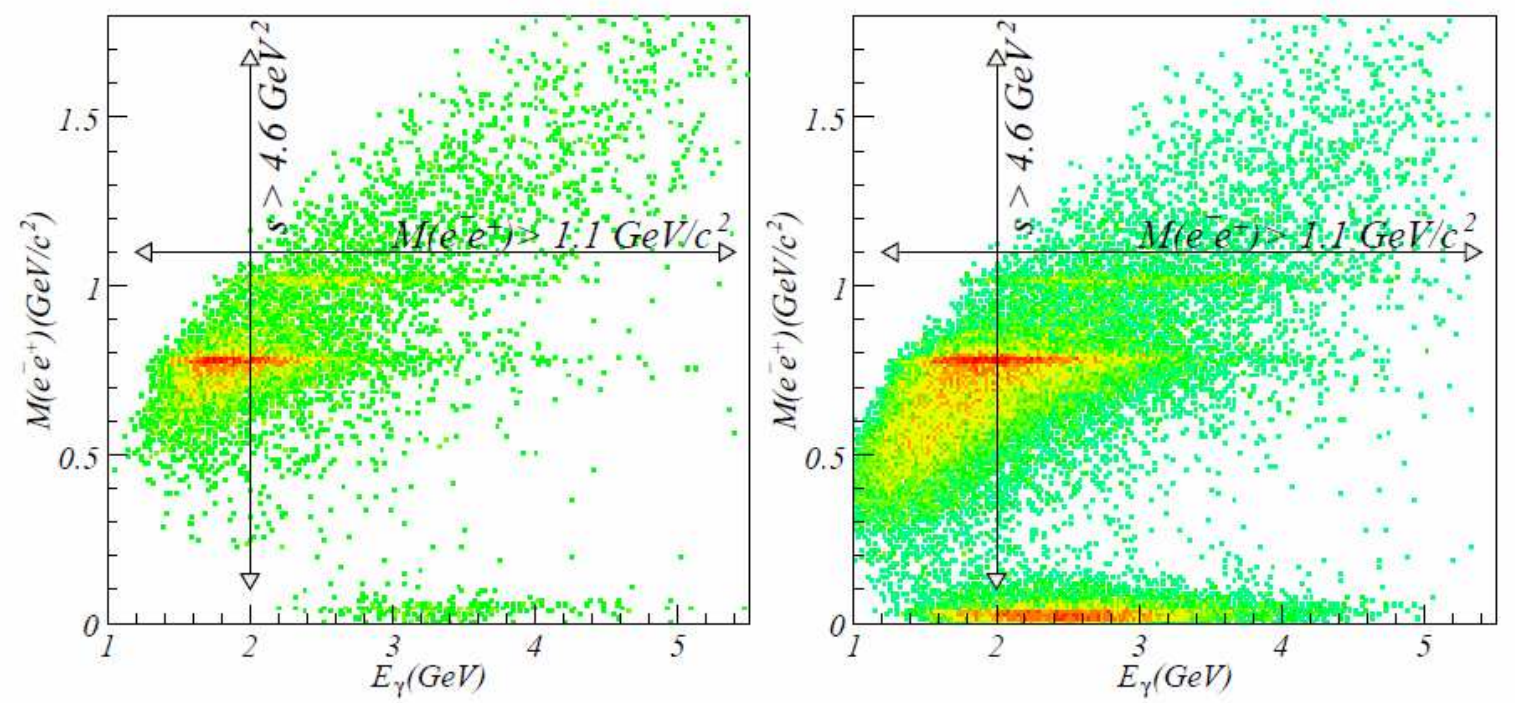

Figure: e^+e^- invariant mass distribution vs quasi-real photon energy. For TCS analysis $M(e^+e^-) > 1.1\,\mathrm{GeV}$ and $s_{\gamma p} > 4.6\,\mathrm{GeV}^2$ regions are chosen. Left graph represents e1-6 data set, right one is from e1f data set.

There is more data from g12 data set, soon to be analyzed. 12 GeV upgrade enables exploration of invariant masses up to $Q^2 = 9\,\mathrm{GeV}^2$ mass.

Theory vs experiment

R.Paremuzyan and V.Guzey:

$$R = \frac{\int d\phi \ \cos\phi \ d\sigma}{\int \ d\phi \ d\sigma}$$

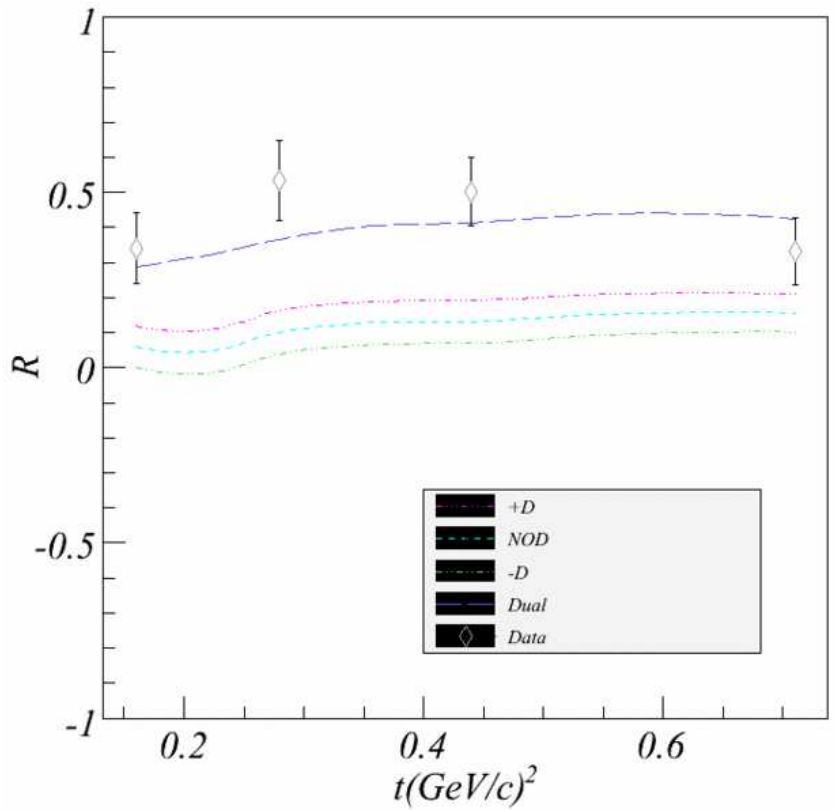

Figure: Theoretical prediction of the ratio R for various GPDs models.

Motivation for NLO

Why do we need NLO corrections to TCS:

- gluons enter at NLO,
- DIS versus Drell-Yan: big K-factors $\log \frac{-Q^2}{\mu_F^2} \to \log \frac{Q^2}{\mu_F^2} \pm i\pi,$
- reliability of the results, factorization scale dependence,

Belitsky, Mueller, Niedermeier, Schafer, Phys.Lett.B474 ,2000.
Pire, L.Sz., Wagner, Phys.Rev.D83, 2011.

General Compton Scattering:

$$\gamma^*(q_{in})N \to \gamma^*(q_{out})N'$$

- DVCS: $q_{in}^2 < 0\,, \quad q_{out}^2 = 0$
- TCS: $q_{in}^2 = 0\,, \quad q_{out}^2 > 0$
- DDVCS: $q_{in}^2 < 0\,, \quad q_{out}^2 > 0$

Amplitude:

$$\begin{aligned}\mathcal{A}^{\mu\nu} &= -g_T^{\mu\nu}\int_{-1}^{1}dx\left[\sum_q^{n_F} T^q(x)F^q(x)+T^g(x)F^g(x)\right]\\ &+ i\epsilon_T^{\mu\nu}\int_{-1}^{1}dx\left[\sum_q^{n_F}\widetilde{T}^q(x)\widetilde{F}^q(x)+\widetilde{T}^g(x)\widetilde{F}^g(x)\right],\end{aligned}$$

$$\begin{aligned}T^q(x) &= \left[C_0^q(x)+C_1^q(x)+\ln\left(\frac{Q^2}{\mu_F^2}\right)\cdot C_{coll}^q(x)\right]-(x\to -x),\\ T^g(x) &= \left[C_1^g(x)+\ln\left(\frac{Q^2}{\mu_F^2}\right)\cdot C_{coll}^g(x)\right]+(x\to -x),\\ \widetilde{T}^q(x) &= \left[\widetilde{C}_0^q(x)+\widetilde{C}_1^q(x)+\ln\left(\frac{Q^2}{\mu_F^2}\right)\cdot \widetilde{C}_{coll}^q(x)\right]+(x\to -x),\\ \widetilde{T}^g(x) &= \left[\widetilde{C}_1^g(x)+\ln\left(\frac{Q^2}{\mu_F^2}\right)\cdot \widetilde{C}_{coll}^g(x)\right]-(x\to -x).\end{aligned}$$

Diagrams

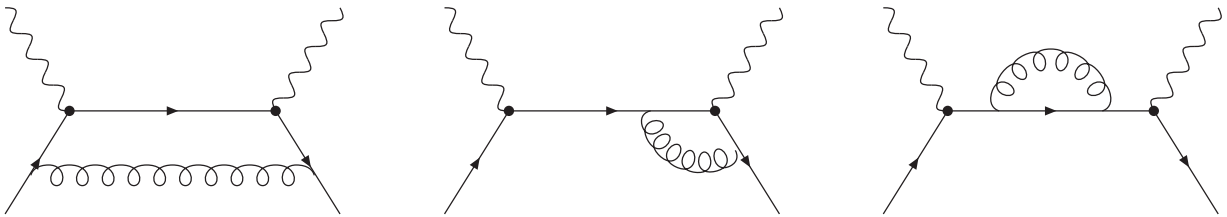

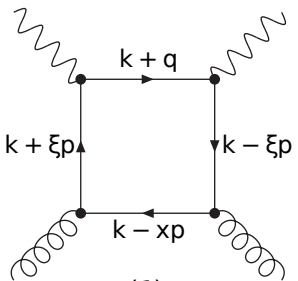

(1)

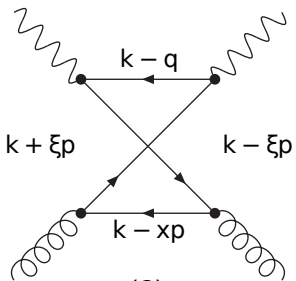

(2)

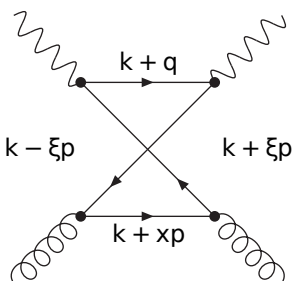

(3)

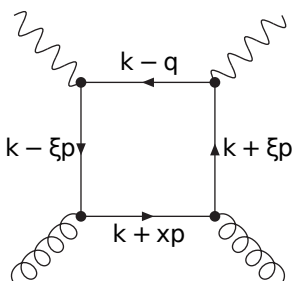

(4)

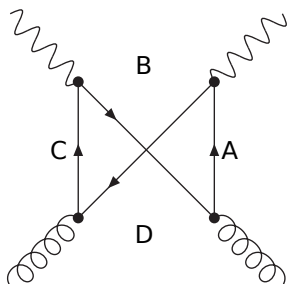

(5)

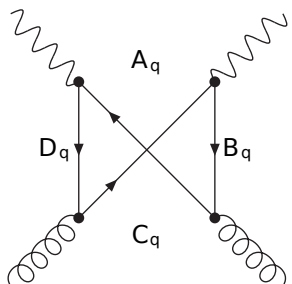

(6)

Results: TCS + DVCS + DDVCS

DVCS:
Quark coefficient functions:

$$
\begin{aligned}
C_0^q(x,\xi) &= -e_q^2 \frac{1}{x+\xi-i\varepsilon}\,, \\
C_1^q(x,\xi) &= \frac{e_q^2\alpha_S C_F}{4\pi}\frac{1}{x+\xi-i\varepsilon}\left[9-3\frac{x+\xi}{x-\xi}\log(\frac{x+\xi}{2\xi}-i\varepsilon)-\log^2(\frac{x+\xi}{2\xi}-i\varepsilon)\right], \\
C_{coll}^q(x,\xi) &= \frac{e_q^2\alpha_S C_F}{4\pi}\frac{1}{x+\xi-i\varepsilon}\left[-3-2\log(\frac{x+\xi}{2\xi}-i\varepsilon)\right], \\
\widetilde{C}_0^q(x,\xi) &= -e_q^2 \frac{1}{x+\xi-i\varepsilon}\,, \\
\widetilde{C}_1^q(x,\xi) &= \frac{e_q^2\alpha_S C_F}{4\pi}\frac{1}{x+\xi-i\varepsilon}\left[9-\frac{x+\xi}{x-\xi}\log(\frac{x+\xi}{2\xi}-i\varepsilon)-\log^2(\frac{x+\xi}{2\xi}-i\varepsilon)\right], \\
\widetilde{C}_{coll}^q(x,\xi) &= \frac{e_q^2\alpha_S C_F}{4\pi}\frac{1}{x+\xi-i\varepsilon}\left[-3-2\log(\frac{x+\xi}{2\xi}-i\varepsilon)\right],
\end{aligned}
$$

where $C_F = (N_c^2-1)/(2N_c)$

DVCS
Gluon coefficient functions:

$$
\begin{aligned}
C_1^g(x,\xi) &= \frac{\Sigma e_q^2 \alpha_S T_F}{4\pi} \frac{1}{(x+\xi-i\varepsilon)(x-\xi+i\varepsilon)} \times \\
&\left[2\frac{x+3\xi}{x-\xi} \log\left(\frac{x+\xi}{2\xi} - i\varepsilon\right) - \frac{x+\xi}{x-\xi} \log^2\left(\frac{x+\xi}{2\xi} - i\varepsilon\right) \right], \\
C_{coll}^g(x,\xi) &= \frac{\Sigma e_q^2 \alpha_S T_F}{4\pi} \frac{2}{(x+\xi-i\varepsilon)(x-\xi+i\varepsilon)} \left[-\frac{x+\xi}{x-\xi} \log\left(\frac{x+\xi}{2\xi} - i\varepsilon\right) \right], \\
\widetilde{C}_1^g(x,\xi) &= \frac{\Sigma e_q^2 \alpha_S T_F}{4\pi} \frac{1}{(x+\xi-i\varepsilon)(x-\xi+i\varepsilon)} \times \\
&\left[-2\frac{3x+\xi}{x-\xi} \log\left(\frac{x+\xi}{2\xi} - i\varepsilon\right) + \frac{x+\xi}{x-\xi} \log^2\left(\frac{x+\xi}{2\xi} - i\varepsilon\right) \right], \\
\widetilde{C}_{coll}^g(x,\xi) &= \frac{\Sigma e_q^2 \alpha_S T_F}{4\pi} \frac{2}{(x+\xi-i\varepsilon)(x-\xi+i\varepsilon)} \left[\frac{x+\xi}{x-\xi} \log\left(\frac{x+\xi}{2\xi} - i\varepsilon\right) \right],
\end{aligned}
$$

where $T_F = \frac{1}{2}$

Discussion

D. Mueller, B. Pire, L. Sz. and J. Wagner, Phys. Rev. D 86 (2012)

The relation between the coefficient functions for
NLO TCS and NLO DVCS:

$$
\begin{aligned}
{}^{TCS}T^{q} &= {}^{DVCS}T^{q\,*} - i\pi\, {}^{DVCS}C^{q\,*}_{coll} \\
{}^{TCS}T^{g} &= {}^{DVCS}T^{g\,*} - i\pi\, {}^{DVCS}C^{g\,*}_{coll}\,.
\end{aligned}
$$

Models for GPDs

Double distribution + D-term

Müller 94, Ji 97, Radyushkin 97, Polyakov, Weiss 99

$$F_i(x,\xi,t) = \int_{-1}^{1} d\beta \int_{-1+|\beta|}^{1-|\beta|} d\alpha\, \delta(\beta+\xi\alpha-x)\, f_i(\beta,\alpha,t) + D_i^F\left(\frac{x}{\xi},t\right)\Theta(\xi^2-x^2)\,,$$

- the polynomiality (Lorentz inv.) of the Mellin moments satisfied authomatically

Models for GPDs

Double distribution + D-term

Müller 94, Ji 97, Radyushkin 97, Polyakov, Weiss 99

$$F_i(x,\xi,t) = \int_{-1}^{1} d\beta \int_{-1+|\beta|}^{1-|\beta|} d\alpha\, \delta(\beta+\xi\alpha-x)\, f_i(\beta,\alpha,t) + D_i^F\left(\frac{x}{\xi},t\right)\Theta(\xi^2-x^2)\,,$$

- the polynomiality (Lorentz inv.) of the Mellin moments satisfied authomatically
- models for DD $f_i(\beta,\alpha,t)$:

$$f_i(\beta,\alpha,t) = g_i(\beta,t)\, h_i(\beta)\, \frac{\Gamma(2n_i+2)}{2^{2n_i+1}\Gamma^2(n_i+1)}\, \frac{[(1-|\beta|)^2-\alpha^2]^{n_i}}{(1-|\beta|)^{2n_i+1}}\,,$$

the profile function $h_i(\beta)$ related to forward PDF e.g. $h^q_{\rm val}(\beta) = q_{\rm val}(\beta)\,\Theta(\beta)$

$g_i(\beta,t)$ controls $t-$dependence of GPDs

Models for GPDs

Our predictions are based on two models of GPDs:

- Goloskokov-Kroll (GK) model

CTEQ6m PDFs and Regge type t-dependence $g_i(\beta,t) = \mathrm{e}^{b_i t}\,|\beta|^{-\alpha_i' t}$

- model based on MSTW08 PDFs and on nucleon e-m. FFs

$$\begin{aligned} g_u(\beta,t) &= \frac{1}{2}F_1^u(t)\,, \\ g_d(\beta,t) &= F_1^d(t)\,, \\ g_s(\beta,t) &= g_g(\beta,t) = F_D(t)\,, \end{aligned}$$

where

$$\begin{aligned} F_1^u(t) &= 2F_1^p(t) + F_1^n(t)\,, \\ F_1^d(t) &= F_1^p(t) + 2F_1^n(t)\,, \\ F_D(t) &= (1 - t/M_V^2)^{-2}\,, \end{aligned}$$

D-term: from chiral soliton model Kivel et al 2001

TCS: Re vs. Im parts of TCS FF MSTW08

H. Moutarde, B. Pire, F. Sabatie, L.Sz. and J. Wagner, "On timelike and spacelike deeply virtual Compton scattering at next to leading order," Phys. Rev. D 87 (2013)

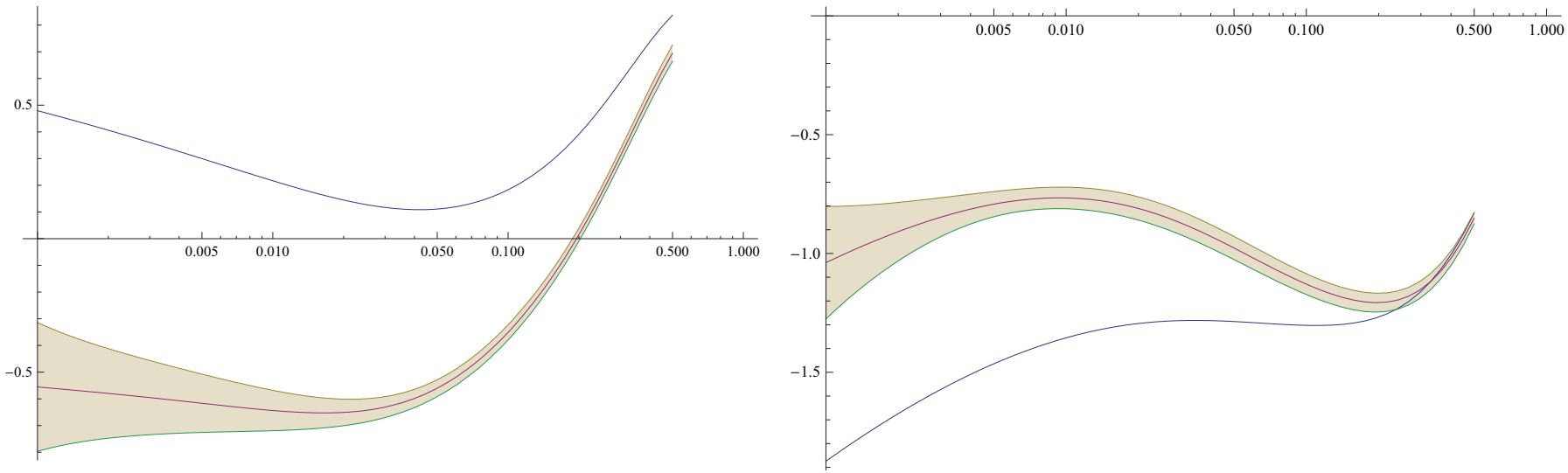

Figure: The real (left) and imaginary(right) parts of the TCS Compton Form Factor $\mathcal{H}$ multiplied by ξ, as a function of ξ in the double distribution model based on MSTW08 parametrization, for $\mu_F^2 = Q^2 = 4$ GeV^2 and $t = -0.1$ GeV^2.

LO : solid line Full NLO : shaded band

(one sigma uncertainty of the input MSTW08 fit to the parton distributions)

TCS: LO vs. NLO-quark vs. NLO-gluon MSTW08

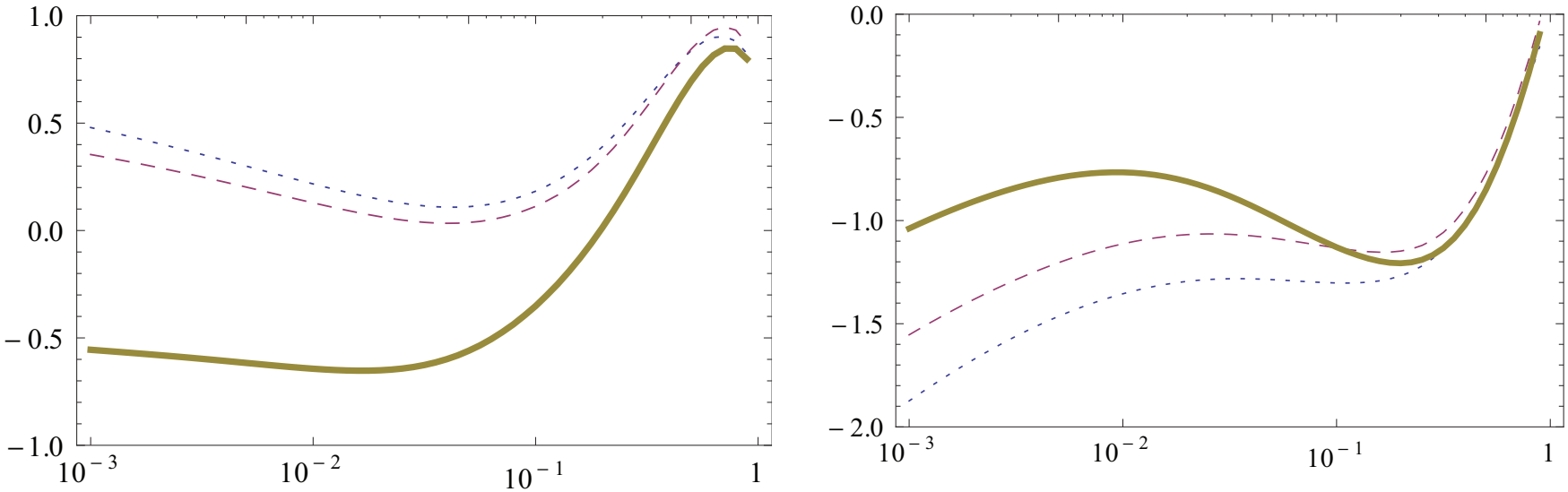

Figure: The real (left) and imaginary(right) parts of the TCS Compton Form Factor $\mathcal{H}$ multiplied by ξ, as a function of ξ in the double distribution model based on MSTW08 parametrization, for $\mu_F^2 = Q^2 = 4$ GeV^2 and $t = -0.1$ GeV^2.

LO : dotted line

LO + NLO-quark : dashed line

LO + NLO-quark + NLO-gluon: solid line

TCS: GK vs MSTW

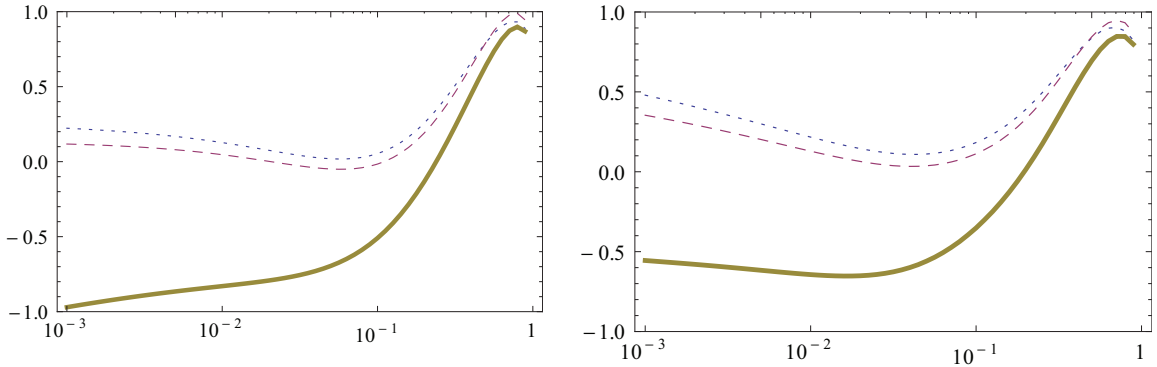

Figure: The real parts of the TCS Compton Form Factor $\mathcal{H}$ multiplied by ξ, as a function of ξ in the double distribution model, for $\mu_F^2 = Q^2 = 4$ GeV^2 and $t = -0.1$ GeV^2.

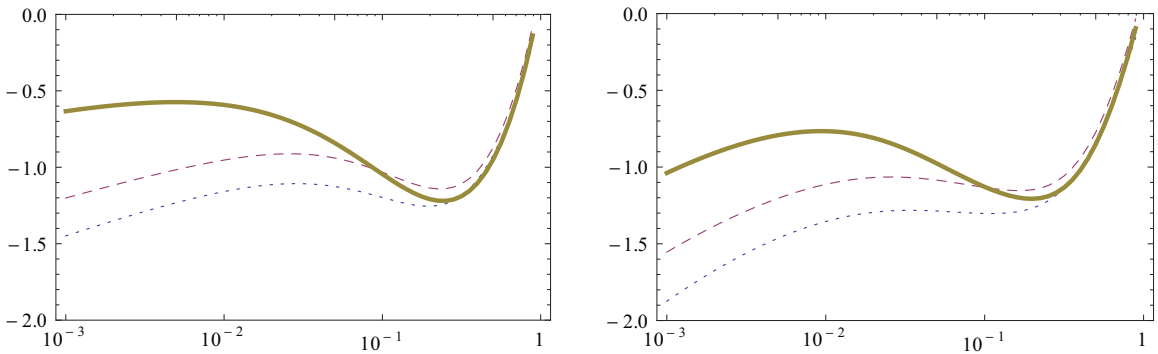

Figure: The imaginary parts of the TCS Compton Form Factor $\mathcal{H}$ multiplied by ξ, as a function of ξ in the double distribution model, for $\mu_F^2 = Q^2 = 4$ GeV^2 and $t = -0.1$ GeV^2.

LO: dotted line LO + NLO-quark: dashed line LO + NLO-quark +NLO-gluon: solid line

Observables

These CFFs are the GPD dependent quantities which enter the scattering amplitudes

For DVCS they are defined as

$$\mathcal{A}^{\mu\nu}(\xi,t) = -e^2 \frac{1}{(P+P')^+}\,\bar{u}(P')\left[g_T^{\mu\nu}\left(\mathcal{H}(\xi,t)\,\gamma^+ + \mathcal{E}(\xi,t)\,\frac{i\sigma^{+\rho}\Delta_\rho}{2M}\right) + i\epsilon_T^{\mu\nu}\left(\widetilde{\mathcal{H}}(\xi,t)\,\gamma^+\gamma_5 + \widetilde{\mathcal{E}}(\xi,t)\,\frac{\Delta^+\gamma_5}{2M}\right)\right] u(P)$$

Similar relation holds for TCS with ξ replaced by η.

DVCS: Observables for JLab

GK model

$d\sigma(l_+) + d\sigma(l_-)$ $d\sigma(l_-) - d\sigma(l_+)$ Asymmetry

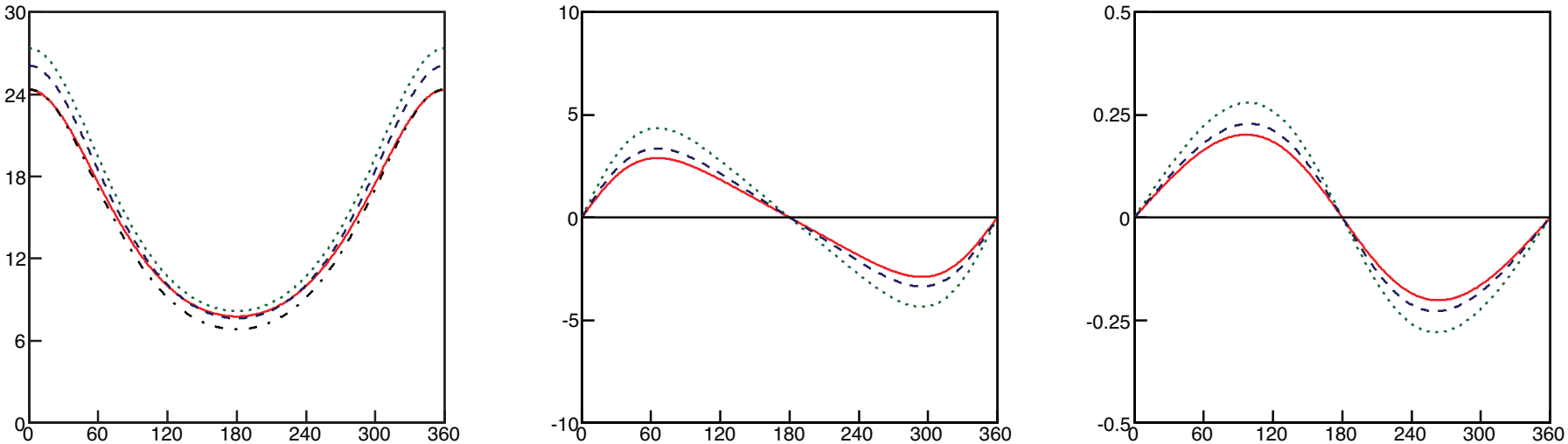

Figure: From left to right, the total DVCS cross section in pb/GeV^4, the difference of cross sections for opposite lepton helicities in pb/GeV^4, the corresponding asymmetry, all as a function of the usual ϕ angle (in Trento conventions) for E_e = 11 GeV; $\mu_F^2 = Q^2$ = 4 GeV^2 and t = - 0.2 GeV^2.

BH (left plot): dash-dotted line

LO: dotted line LO + NLO-quark: dashed line LO + NLO-quark +NLO-gluon: solid line

TCS: Observables for JLab@12GeV

Cross-section:

fixed $t = -0.2\text{GeV}^2$ fixed $\eta = 0.11$

LO: dotted line LO + full NLO : solid line BH (right plot): dashed line

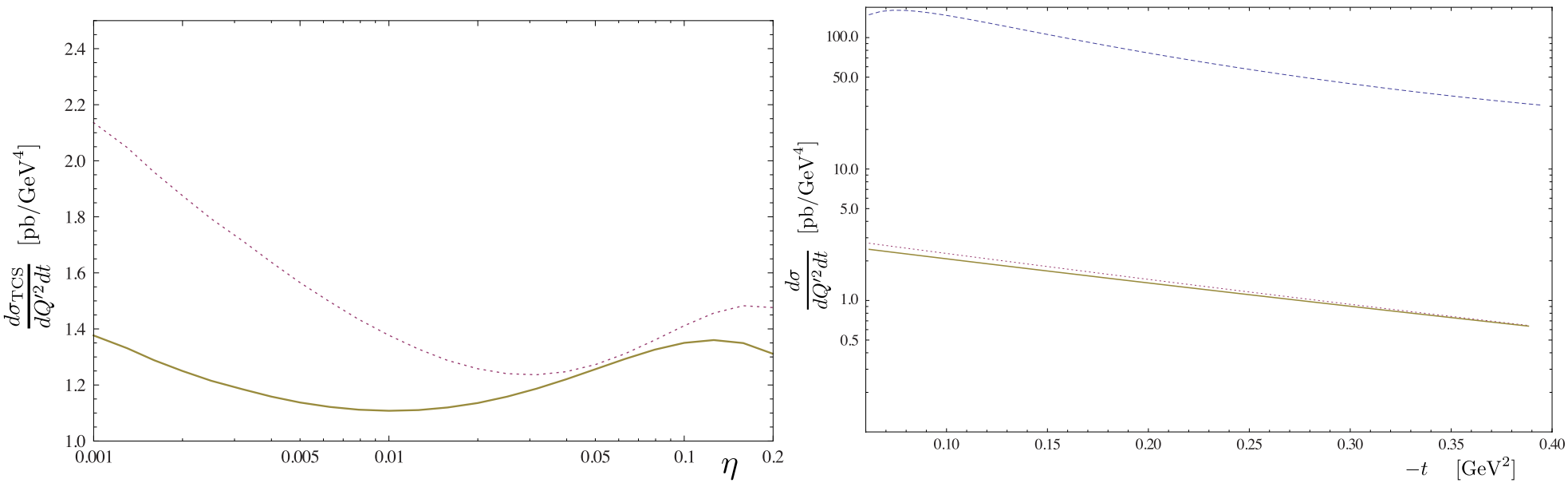

Figure: left : TCS contribution to the cross-section as a function of η for $Q^2 = \mu^2 = 4$ GeV^2, and $t = -0.2$ GeV^2 integrated over $\theta \in (\pi/4, 3\pi/4)$ and over $\phi \in (0, 2\pi)$. Right : TCS and Bethe-Heitler contributions to the cross-section as a function of t for $Q^2 = \mu^2 = 4$ GeV^2 integrated over $\theta \in (\pi/4, 3\pi/4)$ and over $\phi \in (0, 2\pi)$ for $E_\gamma = 10\,\text{GeV}$ ($\eta \approx 0.11$).

large BH $\Rightarrow$ need for more differential observables

TCS: Observables for JLab@12GeV

Azimuthal-dependent cross-section:

pure BH: dashed line BH + Int LO: dotted line BH + Int NLO : solid line

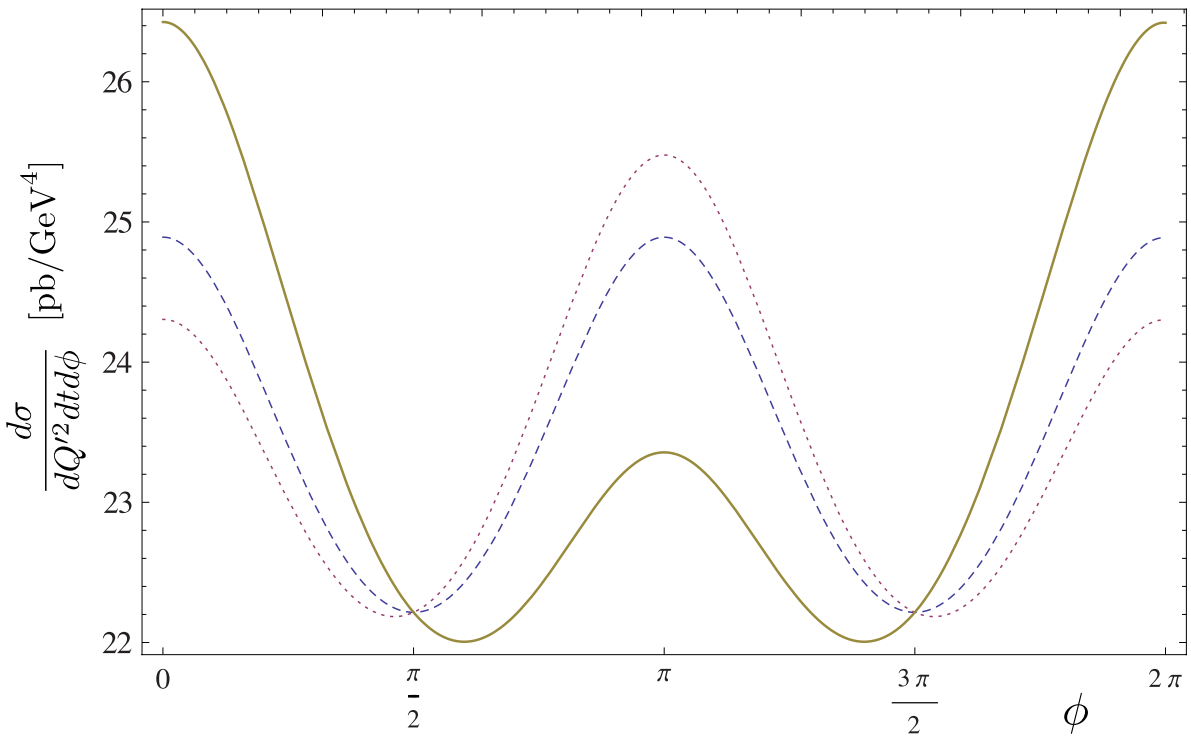

Figure: The ϕ dependence of the cross-section at $E_\gamma = 10$ GeV, $Q^2 = \mu^2 = 4$ GeV^2, and $t = -0.1$ GeV^2 integrated over $\theta \in (\pi/4, 3\pi/4)$.

TCS: Observables for JLab@12GeV

Observable linear in $Re\mathcal{H}$:

$$R(\eta) = \frac{2\int_0^{2\pi} d\phi\, cos\phi\, \frac{d\sigma}{dQ^2\, dt\, d\phi}}{\int_0^{2\pi} d\phi \frac{d\sigma}{dQ^2\, dt\, d\phi}}$$

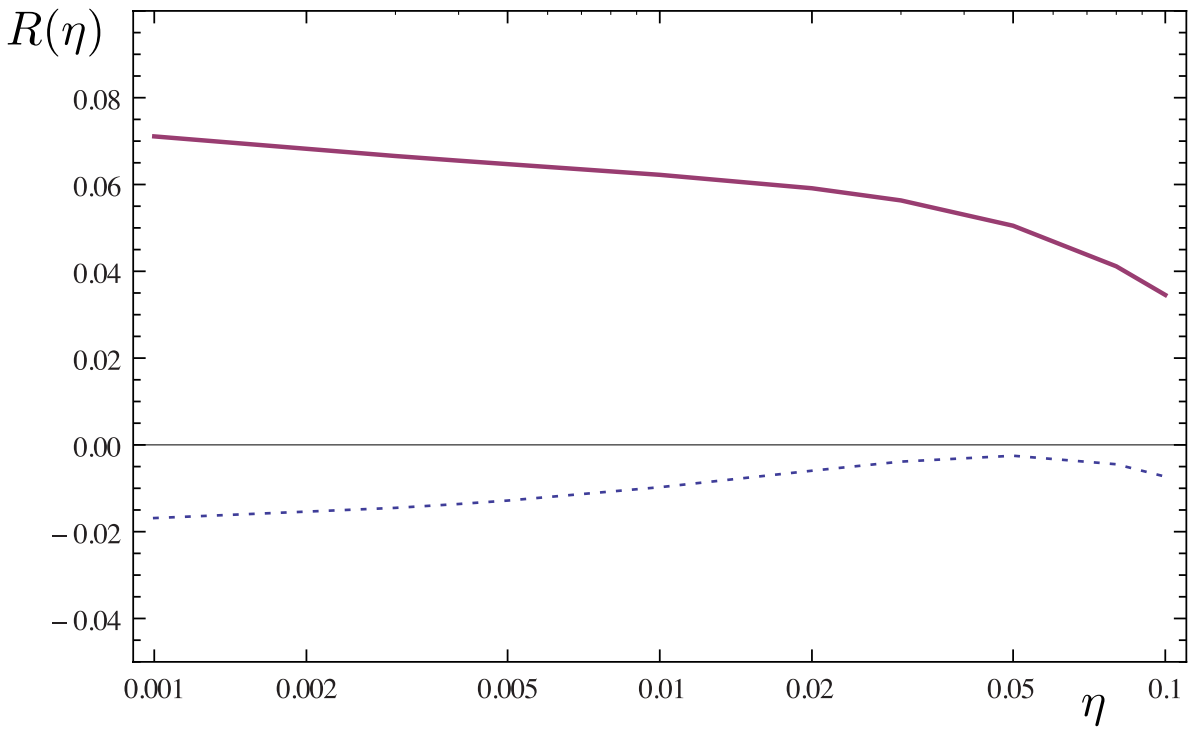

Figure: Ratio R as a function of η, for $Q^2 = \mu_F^2 = 4$ GeV^2 and $t = -0.1$ GeV^2.
LO: dotted line NLO: solid line.

Ultraperipheral collisions

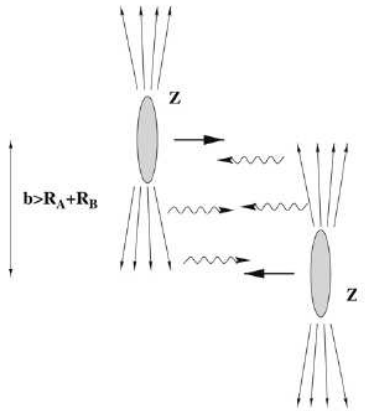

$$\sigma_{pp} = 2 \int \frac{dn(k)}{dk} \sigma_{\gamma p}(k) dk$$

$\sigma_{\gamma p}(k)$ is the cross section for the $\gamma p \to p l^+ l^-$ process and k is the γ's energy, and $\frac{dn(k)}{dk}$ is an equivalent photon flux.

For $\theta = [\pi/4, 3\pi/4]$, $\phi = [0, 2\pi]$, $t = [-0.05\,\mathrm{GeV}^2, -0.25\,\mathrm{GeV}^2]$, $Q'^2 = [4.5\,\mathrm{GeV}^2, 5.5\,\mathrm{GeV}^2]$, and photon energies $k = [20, 900]\,\mathrm{GeV}$ we get:

$$\sigma_{pp}^{BH} = 2.9\mathrm{pb}\ .$$

The Compton contribution gives:

$$\sigma_{pp}^{TCS} = 1.9\mathrm{pb}\ .$$

The interference cross section

B. Pire, L.Sz, J. Wagner, Phys. Rev. D (2009)

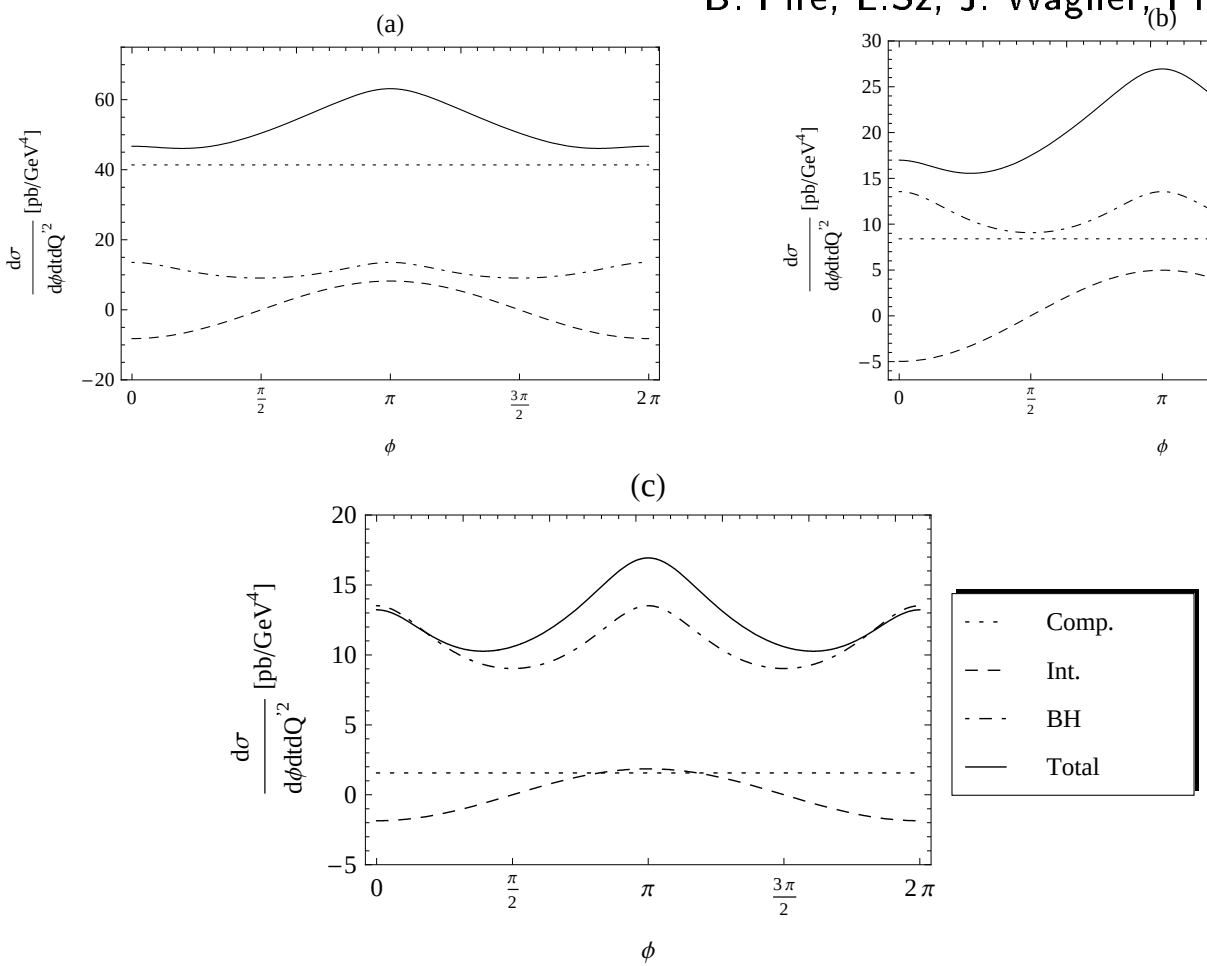

Figure: The differential cross sections (solid lines) for $t = -0.2\,\mathrm{GeV}^2$, $Q'^2 = 5\,\mathrm{GeV}^2$ and integrated over $\theta = [\pi/4, 3\pi/4]$, as a function of φ, for $s = 10^7\,\mathrm{GeV}^2$ (a), $s = 10^5\,\mathrm{GeV}^2$(b), $s = 10^3\,\mathrm{GeV}^2$ (c) with $\mu_F^2 = 5\,\mathrm{GeV}^2$.

Ultraperipheral collisions at RHIC

$L \cdot k \quad \frac{dn}{dk}(\mathrm{mb}^{-1}\mathrm{sec}^{-1})$

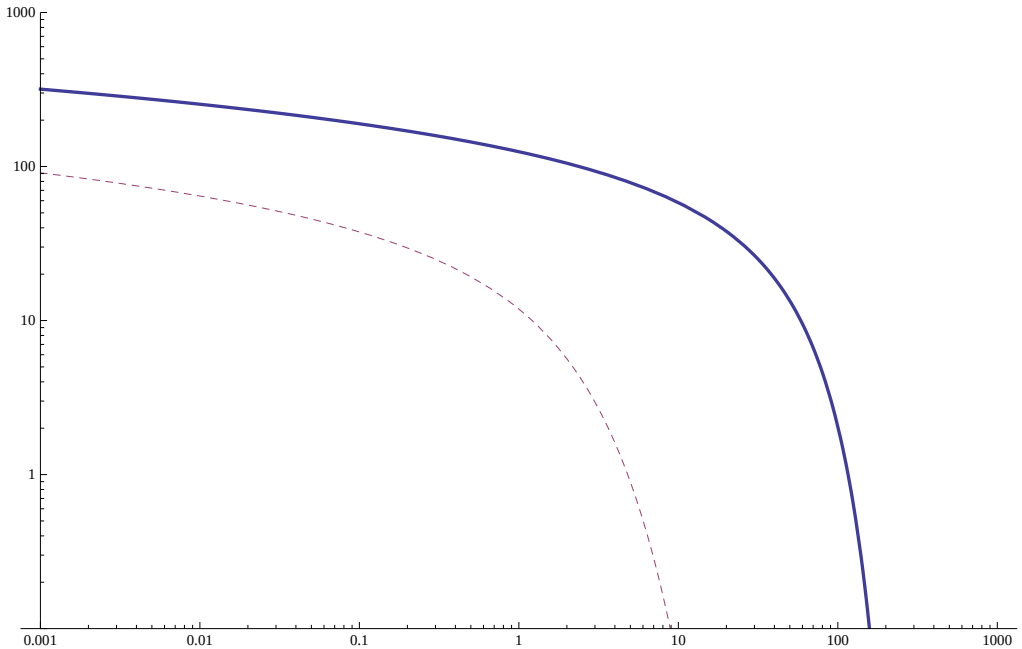

Figure: Effective luminosity of the photon flux as a function of photon energy k(GeV) in
Au-Au (dashed line) and proton-proton (solid line) collisions.

RHIC

$\frac{d\sigma^{AuAu}}{dQ^2 dt d\phi}(\mu\text{b GeV}^{-4})$

J. Wagner

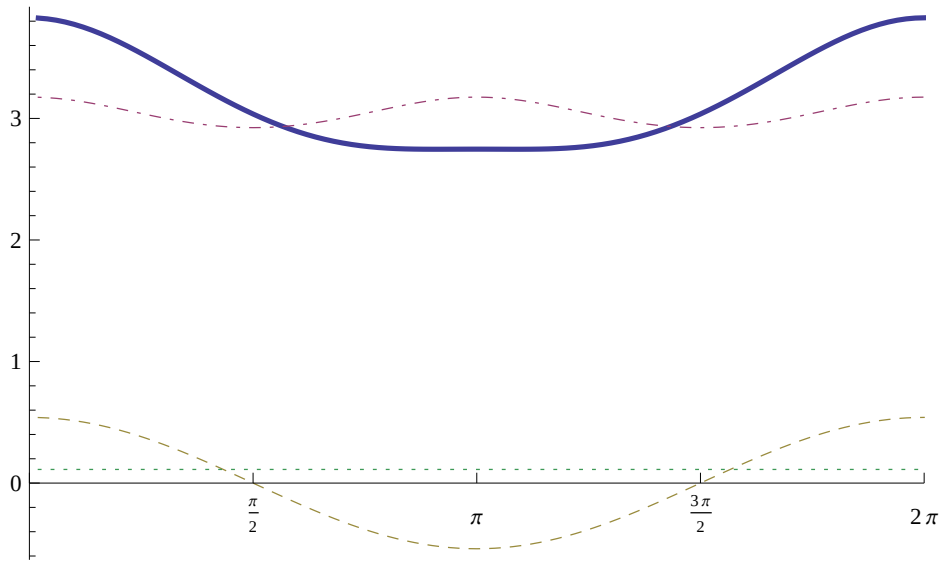

Figure: The differential cross sections (solid lines) for $t = -0.1\,\text{GeV}^2$, $Q'^2 = 5\,\text{GeV}^2$ and integrated over $\theta = [\pi/4, 3\pi/4]$, as a function of φ.

Compton: dotted line, B-H: dash-dotted line and Interfer.: dashed line

Total BH cross section (for $Q \in (2, 2.9)\,\text{GeV}$, $t \in (-0.2, -0.05)\,\text{GeV}^2$, $\theta = [\pi/4, 3\pi/4]$ and $\phi \in (0, 2\pi)$)

$$\sigma_{BH} = 41\mu\text{b} \qquad \text{Rate} = 0.04\text{Hz}$$

RHIC

$\frac{d\sigma^{pp}}{dQ^2 dt d\phi}(\text{pb GeV}^{-4})$

J. Wagner

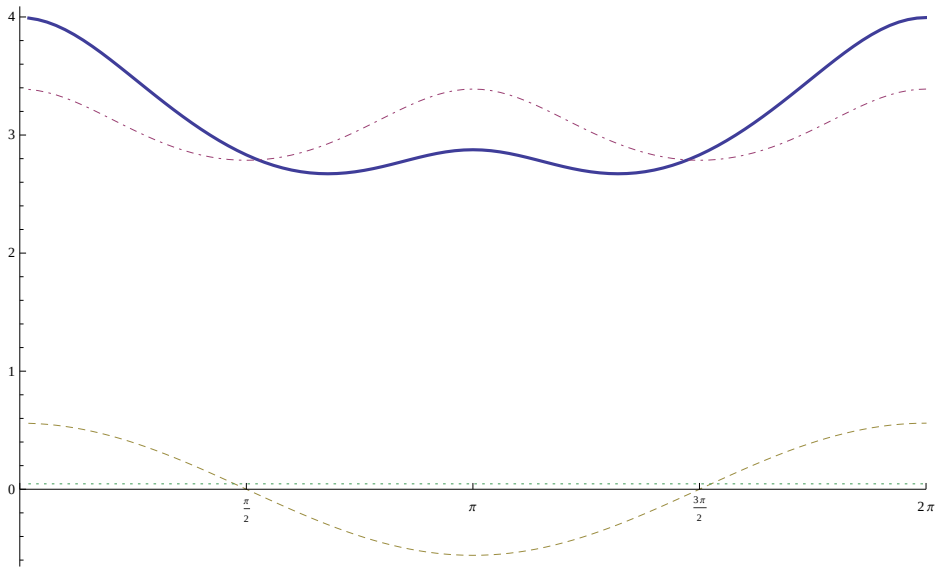

Figure: The differential cross sections (solid lines) for $t = -0.1\,\text{GeV}^2$, $Q'^2 = 5\,\text{GeV}^2$ and integrated over $\theta = [\pi/4, 3\pi/4]$, as a function of φ.

Compton: dotted line, B-H: dash-dotted line and Interf.: dashed line

Total BH cross section (for $Q \in (2, 2.9)\,\text{GeV}$, $t \in (-0.2, -0.05)\,\text{GeV}^2$, $\theta = [\pi/4, 3\pi/4]$ and $\phi \in (0, 2\pi)$)

$$\sigma_{BH} = 9\text{pb} \qquad \text{Rate} = 5/\text{day}$$

DVCS: factor. scale dependence $Q^2 = 4\text{GeV}^2$, $t = -0.1\text{GeV}^2$, $\alpha_s = 0.3$

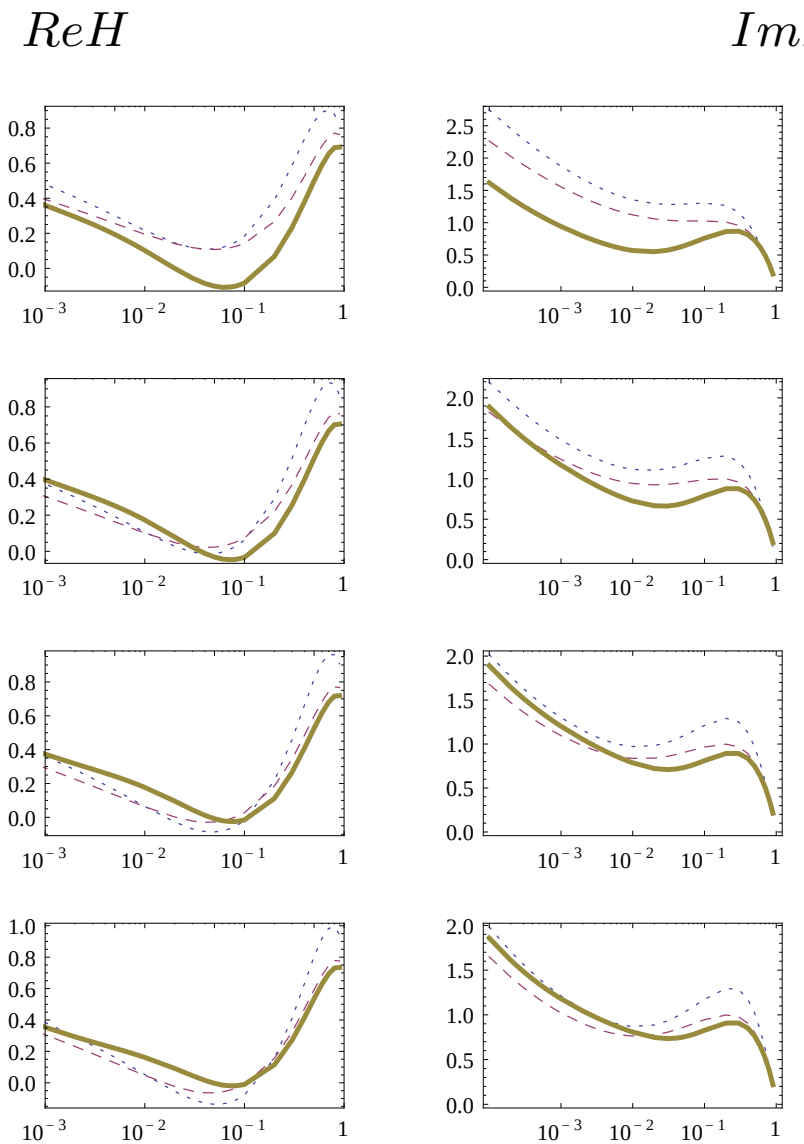

Figure: dotted - LO, dashdotted - NLO (quarks), solid - Full NLO, rows: $\mu^2 = Q^2$, $\mu^2 = Q^2/2$, $\mu^2 = Q^2/3$, $\mu^2 = Q^2/4$,

DVCS: factor. scale dependence $Q^2 = 4\text{GeV}^2$, $t = -0.1\text{GeV}^2$, $\alpha_s = 0.3$

Full NLO

ReH ImH

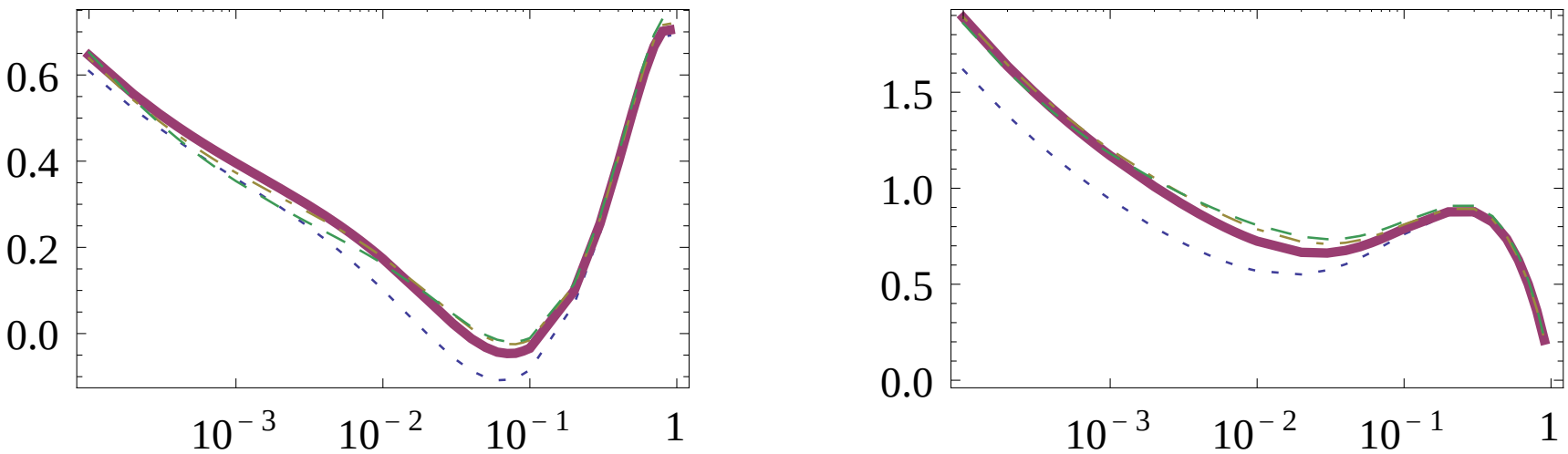

Figure:
dotted: $\mu^2 = Q^2$, solid: $\mu^2 = Q^2/2$, dashdotted: $\mu^2 = Q^2/3$, dashed: $\mu^2 = Q^2/4$,

DVCS: factor. scale dependence $Q^2 = 4\text{GeV}^2$, $t = -0.1\text{GeV}^2$, $\alpha_s = 0.3$

LO vs. Full NLO

ReH

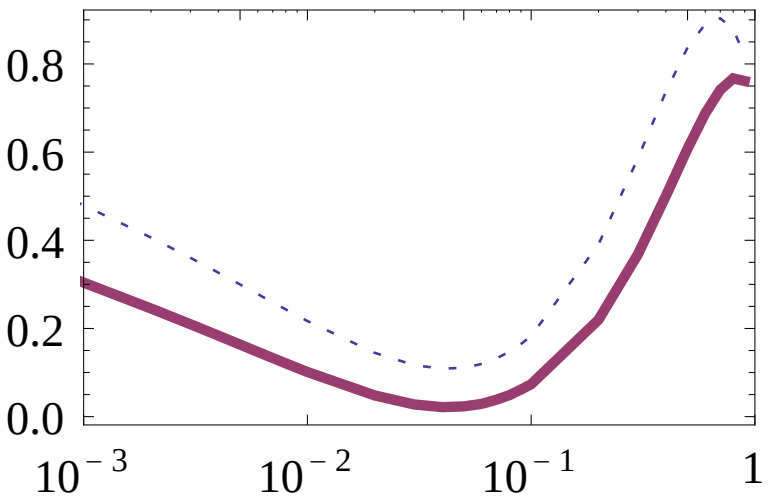

ImH

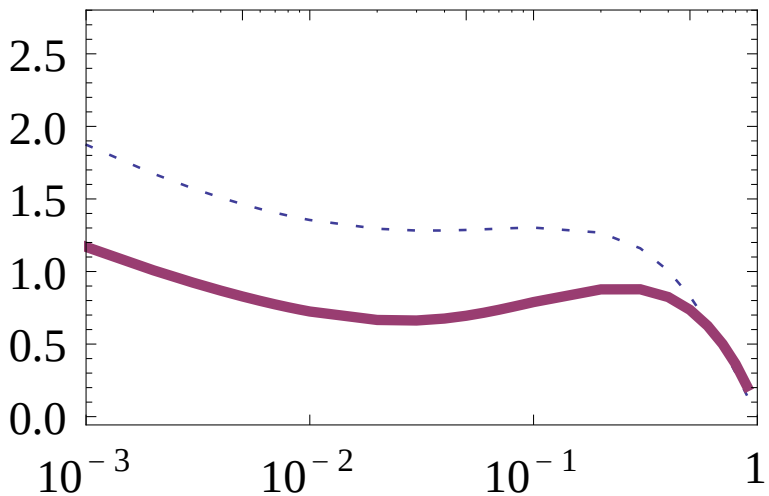

Figure: dotted: LO $Q^2 = \mu^2$, solid: NLO $Q^2 = 2\mu^2$,

TCS: factor. scale dependence $Q^2 = 4\text{GeV}^2$, $t = -0.1\text{GeV}^2$, $\alpha_s = 0.3$

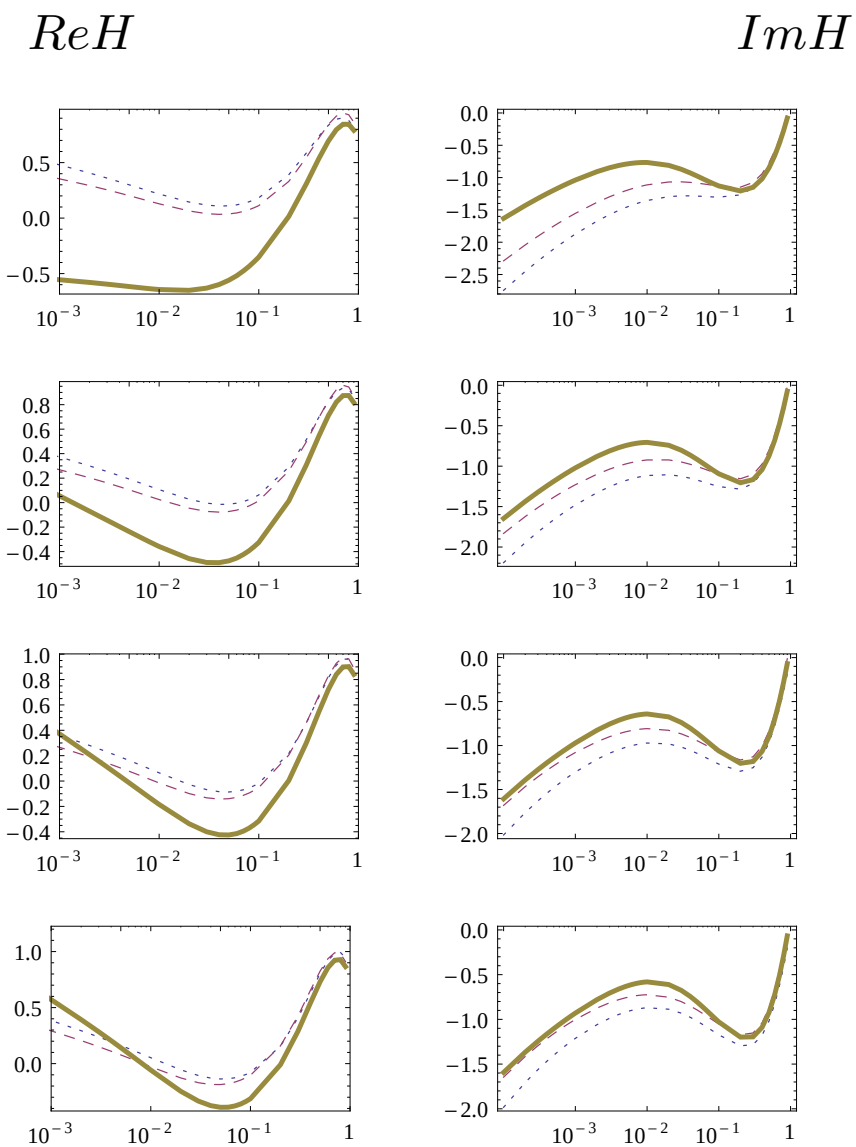

Figure: dotted - LO, dashdotted - NLO (quarks), solid - Full NLO,
rows: $\mu^2 = Q^2$, $\mu^2 = Q^2/2$, $\mu^2 = Q^2/3$, $\mu^2 = Q^2/4$,

TCS: factor. scale dependence $Q^2 = 4\text{GeV}^2$, $t = -0.1\text{GeV}^2$, $\alpha_s = 0.3$

Full NLO

ReH ImH

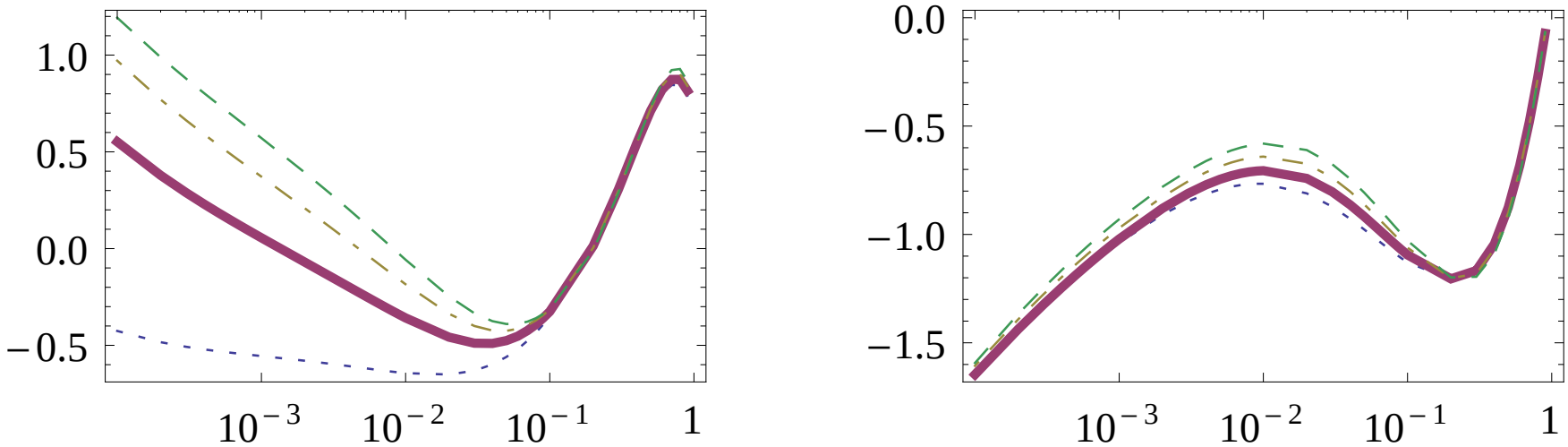

Figure:
dotted: $\mu^2 = Q^2$, solid: $\mu^2 = Q^2/2$, dashdotted: $\mu^2 = Q^2/3$, dashed: $\mu^2 = Q^2/4$,

Summary

- TCS already measured in JLAB 6 GeV, but much richer and more interesting kinematical region available after upgrade to 12 GeV.
- NLO corrections need to be better understood, specially gluon sector,
- Compton scattering in ultraperipheral collisions at hadron colliders opens a new way to measure generalized parton distributions
- TCS is an experimentally challenging study at JLab, COMPASS, RHIC and LHC or AFTER@LHC , in many cases due to limitations of original detectors

MERCI POUR VOTRE ATTENTION !